2Pb2-5

Subband Compound with Harmonics in Plane Wave Beamforming

平面波ビームフォーミングにおける高調波サブバンドコンパウンド

Jie Zheng[1†], Norio Tagawa[1], Masasumi Yoshizawa[2], and Takasuke Irie[1,3]
([1]Tokyo Metropolitan University; [2]Tokyo Metropolitan College of Industrial Technology ; [3]Microsonic Co, Ltd.)
鄭傑 [1†], 田川憲男 [1], 吉澤昌純 [2], 入江喬介 [1,3] ([1] 東京都立大学, [2] 東京都立産業技術高等専門学校, [3] マイクロソニック(株))

1. Introduction

The use of harmonics contributes to high resolution and low artifact imaging [1]. However, its intensity depends on the depth and is significantly weaker than the fundamental echo, so simultaneous use with the fundamental echo is desired. At present, integrations that are effective for both resolution and SNR have not yet been resolved.

For the fundamental wave, we realized a significant improvement in range resolution by compounding the subbands extracted by filtering with adaptive weighting [2]. In this method, since the subband components are freely extracted and their amplitudes are normalized and used, it can be applied to harmonics without any special change.

However, in order to improve the resolution in the range direction by beamforming, the frequency band used must be as flat and wide as possible. The fundamental and harmonic echoes have separate bands, and if used as they are, they will not meet the above conditions. Therefore, in this study, we propose a method that transmit the pulse twice, where the frequency band of the second incident signal is used to connect the fundamental and harmonic parts of the first received echo. Then, amplitude correction is performed so that the entire band becomes one flat wide band. The entire bandwidth connected by the two fundamentals and one harmonic is then used for the subband compound.

2. Method

In the subband compound, it is easy to control the used band and the FM chirp pulse that is effective from the viewpoint of SNR is used as the transmission signal. An FM chirp pulse is sent using the entire effective band of the probe, and L randomly selected narrowband components are extracted from the received signal. The value corresponding to the pixel to be imaged is extracted from the j-th band component of the echo received by the i-th element of the array probe and set as x_{ij}. It is assumed that the phase shift due to the delay process has been compensated.

First, the variance-covariance matrix $\mathbf{R}_F$ for the frequencies required for the frequency weight calculation is estimated. The snapshot vector $\mathbf{s}_i$ is calculated as follows:

$$(s_i)_j = \frac{1}{N-1}\sum_{k=1,\,k\neq i}^{N} x_{ij}\,,\ i = 1,\cdots,N,\ j = 1,\cdots,L. \qquad (1)$$

$\mathbf{R}_F$ is estimated using the snapshot as follows:

$$\hat{\mathbf{R}}_F = \frac{1}{N}\sum_{i=1}^{N}\mathbf{s}_i\mathbf{s}_i^{\mathrm{H}}\,, \qquad (2)$$

where $^{\mathrm{H}}$ is Hermitian transposition. By the minimum variance criterion, the optimal weight vector is obtained as follows:

$$\mathbf{w}_F = \frac{\mathbf{R}_F^{-1}\mathbf{1}_L}{\mathbf{1}_L^{\mathrm{T}}\mathbf{R}_F^{-1}\mathbf{1}_L},\ \mathbf{1}_L = [1,\cdots,1]^{\mathrm{T}}. \qquad (3)$$

Then, the output of FPWC-MVDR with one wideband transmission y_F is defined as the following equation.

$$y_F = \mathbf{w}_F^{\mathrm{H}}\mathbf{u},\ u_j = \sum_{i=1}^{N} x_{ij}\,. \qquad (4)$$

The pixel value can be calculated as $(y_F{}^*\, y_F)^{1/2}$.

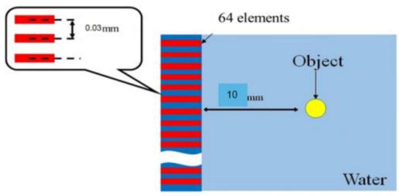

Fig. 1 Experimental setup.

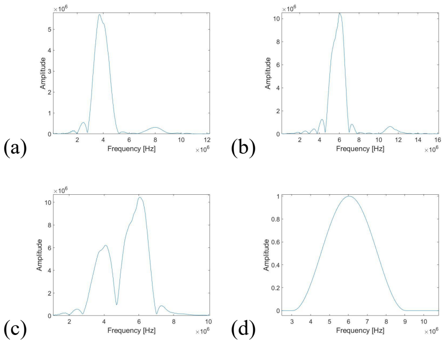

Fig. 2 received echo at (a)4MHz (b)5.7MHz (c)the summed signal from echos and (c)the amplitude corrected signal in entire bandwidth.

3. Simulation

To verify the effectiveness of the proposed method, we used OnScale software which is a standard finite element method (FEM) code for ultrasound propagation to build an experimental environment. The beamforming procedure was performed offline on the ultrasound echoes received by the individual transducer elements. In our simulation, the sampling frequency is 813 MHz and the number of sampling points is 20320.

Figure 1 shows that in this simulation a plane wave was transmitted and the entire array composed of 64 elements received the echo. The element width is 0.04 mm and the pitch is 0.03 mm. Place the target with a diameter of 0.1 mm in the water-filled area 10 mm from the transducer.2 short pulse that is generated with 4 MHz and 5.7MHz frequency 6-cycle form was used as the transmission pulse. In this study, transmission is limited to the front direction. That is, no spatial compound is performed. After the echo signals were obtained from the experimental environment by OnScale software, the signal processing step was performed offline using MATLAB software.

Figures 2(a) and 2(b) shows 2 received echoes with different center frequencies and their respective harmonics in frequency domains. Figure 2(c) shows the summed signal of the echoes in Figs. 2(a) and 2(b). Figure 2(d) shows the amplitude corrected signal in entire bandwidth from the signal of Fig. 2(c). Tthe signal in Fig. 2(d) is divided into 10 subbands with a bandwidth of 1 MHz. The subband positions were confirmed by fixing the overlapping of the subbands to half of the subband bandwidth and varying the numbers of subbands and their bandwidths. In this paper, all observations are treated as analytic signals obtained by quadrature detection of RF signals, that is, IQ (In-phase and Quadrature-phase) signals. Equation 4 is used as a beamformer output with $N = 64$ and $L = 10$.

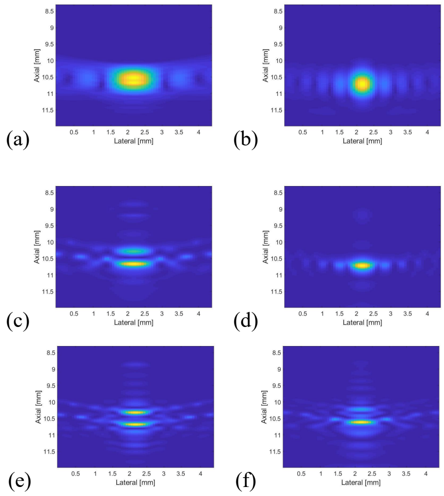

Fig. 3 B-mode image by DAS using (a) fundamental and (b) harmonics ; B-mode images by subband compound using (c) fundamental, (d) harmonic, (e) fundamental and harmonic without amplitude correction and (f) fundamental and harmonic with amplitude correction (proposed).

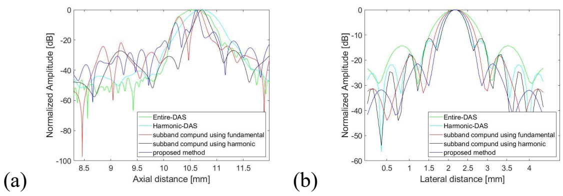

Fig. 4 Amplitude distribution profiles along (a) range direction and (b) lateral direction.

4. Result and Discussion

For comparison, we extracted 10 subbands from the base band (3-9MHz). **Figures 3**(a) to (f) show the B-mode images generated under each condition. **Figures 4** (a) and (b) are their intensity profiles. We can confirm that the amplitude correction can effectively reduce the artifacts (comparing Figs. 3(e) and (f)). Additionally, we can see that the proposed method has a good improvement in axial and lateral resolution and has a low sidelobe level compared others.

5. Conclusion and Future Work

We can already use fundamental echo and harmonic echo through subband compound. In the future, we plan to investigate the relationship between performance and imaging depth, which determines the magnitude of harmonics.

References

1. C-H Nguyen, J. Zhu, N. Tagawa, M. Yoshizawa, T. Irie: Proc. Mtgs. Acoust. **38** (2019) 055009.
2. J. Zheng, N. Tagawa, M. Yoshizawa, T. Irie: Jpn. J. Appl. Phys., **60** (2021) pp.SDDB08-1-15.